Distraction-Aware Drone Path Planning for Construction Safety

Wei Han[1], Liqun Xu[1], Mahfuza Maisha Mouri[2], Wei-Yin Loh[3], Fei Dai[2], Zhenhua Zhu[1]

[1]Department of Civil and Environmental Engineering, University of Wisconsin - Madison, USA
[2]Wadsworth Department of Civil and Environmental Engineering, West Virginia University, USA
[3]Department of Statistics, University of Wisconsin - Madison, USA
whan59@wisc.edu, liqun.xu@wisc.edu, mm00286@mix.wvu.edu, loh@stat.wisc.edu, fei.dai@mail.wvu.edu, zzhu286@wisc.edu

Abstract –

Unmanned aerial vehicles (UAVs) are increasingly used in construction for inspection, monitoring, and safety management. While these applications offer operational benefits, recent studies indicate that drone presence and motion can distract on-site workers and impair situational awareness. Existing construction drone path planning methods, however, primarily emphasize efficiency, coverage, and collision avoidance, with limited consideration of human distraction effects. This study proposes a distraction-aware drone path planning method that explicitly incorporates worker distraction risk into autonomous flight planning. Distraction is modeled as a soft cost within a three-dimensional cost grid, together with hard constraints representing physical obstacles. A local path planning module evaluates motion and distraction-related costs between travel points, while the global visiting sequence is formulated as a Traveling Salesman Problem. A soft cost weight estimation module analytically determines appropriate weighting parameters based on spatial relationships between travel points and worker distraction boundaries. The proposed method was implemented and evaluated in a Unity-based virtual construction environment under multiple flight scenarios. Results show that incorporating distraction-related soft costs reduces the time drones spend within worker distraction areas, with moderate increases in total flight time. These findings demonstrate the feasibility of integrating cognitive safety considerations into construction drone path planning.

Keywords –

Unmanned aerial vehicles (UAVs); Path planning; Worker distraction; Human-centered navigation; Construction safety

1 Introduction

Drone usage in construction projects is gaining significant traction due to its potential to enhance project efficiency, safety, and decision making. Modern drones are equipped with advanced sensing technologies, including RGB, multispectral, thermal, and LiDAR sensors, enabling rapid collection of large-scale aerial data [1]. These data can be transmitted and processed through specialized software to support efficient analysis, site monitoring, and decision making, thereby streamlining workflows, improving site management, and facilitating more comprehensive inspections. Reflecting these advantages, the global construction drone market was valued at approximately $4.8 billion in 2019 and is projected to reach $7.1 billion by 2030 [2]. The expanding technical capabilities of drones, together with strong market growth, indicate their increasing integration into construction practices.

Despite these benefits, the introduction of drones into construction environments may also create new safety risks for workers on site. In particular, drone-induced distraction has the potential to compromise workers' cognitive focus and situational awareness [3]. The presence or movement of drones can divert attention through visual, auditory, or cognitive channels, drawing workers' focus away from critical tasks or surrounding hazards [4]. For example, Union Pacific Corp. railroad workers reported that drones flying over rail yards caused them to look upward rather than concentrate on their duties, even while 200-ton locomotives and railcars were in motion[5]. Prior research in office environments has shown that workers disrupted by external interruptions may require up to 25 minutes to fully regain concentration [6]. Similar effects are likely in construction settings, where sustained attention is essential for safe task execution. Recent studies have confirmed that drones can interrupt construction workers during active job tasks[7] , and such distractions may reduce workers' ability to recognize hazards and accurately assess safety risks [8,9].

Building on this line of inquiry, Han et al. quantitatively examined drone-induced distraction in construction contexts using controlled experimental methods [10,11]. These studies provided empirical evidence that drone presence and flight behaviours can significantly influence workers' situational awareness. However, existing research has primarily focused on measuring and characterizing distraction effects, rather than on developing operational strategies to mitigate them. In particular, existing drone deployment and path-planning approaches in construction primarily account for factors such as task constraint factors [12,13], navigability factors [14,15], and energy efficiency factors [16]. The distraction impact of drone flight paths on workers' attention and safety has not yet been incorporated into these approaches.

To address this gap, this study proposes a distraction-aware drone path planning method for construction environments. The proposed method integrates human attention considerations into the drone path planning process, enabling flight trajectories that balance operational efficiency with reduced distraction to on-site workers. By explicitly accounting for distraction-related costs during path optimization, the approach aims to support safer drone integration into construction workflows while preserving the practical benefits of aerial monitoring and data collection.

2 Literature Review

2.1 Drone Path Planning in Construction

Recent research has increasingly explored drone path planning algorithms to construction applications, aiming to enhance safety, inspection efficiency and automated monitoring as mentioned in section Drone Application in Construction.

For inspection, Xu et al. focused on drone path planning for bridge construction safety inspection by proposing an enhanced Snake optimization algorithm (CSGLSO). This algorithm considered energy efficiency collision avoidance, trajectory smoothness, rapid convergence, and the avoidance of local optima in 3D environments [12]. Zheng et al. proposed a drone-based building facade visual inspection through coverage path planning. Their two-stage framework combined normal vector segmentation, k-means clustering, and greedy optimization for viewpoint generation with a hybrid Ant Colony Optimization and Differential Evolution (DACO-DE) for path planning. The study emphasized complete surface coverage, minimizing redundancy, reducing path length, collision avoidance, smoothness in flight trajectories, and energy efficiency [13].

Moreover, Liu et al. developed a drone-based construction site refinement inspection method integrating BIM and 3D reconstruction. Waypoints were selected using an improved Artificial Potential Field combined with a greedy algorithm, while global path optimization relied on A* and Simulated Annealing. Their method considered obstacle avoidance, low-altitude flight safety, efficient waypoint distribution, image coverage, and energy consumption reduction [14]. Freimuth and König explored drones for construction inspection and structural health monitoring (SHM) within a BIM-integrated workflow. They generated collision-free flight paths using a discretized graph from BIM data and validated navigation strategies with Software-In-The-Loop simulation. The framework considered collision avoidance, battery usage, weather and lighting effects, camera parameters, and overall safety of autonomous drone operations [15].

For monitoring, Huang and Hammad focused on unmanned aerial vehicle-based automated video collection of dynamic construction activities to support progress and safety monitoring. Path optimization was achieved using a Non-Dominated Sorting Genetic Algorithm II, while routing relied on the A-star algorithm and a random-key genetic algorithm. The approach incorporated visual coverage, occlusion avoidance, travel time minimization, collision risk management, integration with four-dimensional Building Information Modeling micro-schedules, and data quality for computer vision processes [16].

2.2 Drone-Induced Distraction

Virtual and augmented reality (VR/AR) experiments provide immersive, controlled environments that allow researchers to safely replicate distractions and measure their impact on attention, performance, and situation awareness. Jeelani et al. used virtual reality to simulate construction sites and assess the impact of drone presence on workers' attention and stress, finding that drones distracted workers at distances of 12 and 25 ft but did not significantly affect psychological distress [17]. Similarly, Albeaino et al. applied VR to examine attentional impacts at varying distances, showing that drones at greater distances elicited longer and more frequent fixations [18].

In transportation, Barlow et al. used a VR driving simulator to show that drones near the roadside distract drivers, recommending a minimum 25 ft buffer [19]. A VR study by the Oregon Department of Transportation found increased glance frequency and unsafe glances (>2 s) at lateral offsets of 0, 25, and 50 ft [20]. Ryan et al. further demonstrated with a simulator using a real vehicle seat that drones caused critically long glances in 11% of cases [21]. Collectively, these studies confirm that VR and simulators are effective tools for assessing drone-induced driver distraction.

3 Method

The proposed drone navigation method is composed of four modules: (1) a 3D cost grid, (2) a local path planning module, (3) a traveling points ordering module, and (4) a soft cost weight estimation module. The 3D cost grid serves as the spatial foundation of the method by representing the construction environment in a discretized three-dimensional structure. Each grid cell encodes two types of information, hard costs and soft costs. Hard costs are defined as non-traversable areas corresponding to physical obstacles. Soft costs represent the distraction risks. Using this grid-based environment model, the local path planning module computes feasible flight paths between any two traveling points. The module evaluates both spatial efficiency and safety by integrating geometric distance, obstacle avoidance, and distraction risk.

A weight factor is introduced to balance efficiency and safety within the soft-cost function. Higher weights place greater emphasis on safety over efficiency. The soft-cost weight estimation module determines the appropriate weight based on the spatial relationships between travel points and distraction areas. These computed costs are then passed to the travel point ordering module, which identifies the optimal visiting sequence to reduce the overall travel cost. Finally, the routes between consecutive points are combined to generate a complete navigation path that enables the drone to visit all target locations efficiently while avoiding obstacles and minimizing exposure to high-risk distraction zones.

3.1 3D Cost Grid Module

The 3D Cost Grid Module provides the spatial foundation for the drone navigation method by discretizing the construction site into a structured three-dimensional grid. Each grid cell $G(i,j,k)$ represents a voxel of the environment with dimensions defined by the grid resolution R. Within this grid, environmental objects such as workers, cranes, and static structures are projected according to their physical boundaries. The cost of each cell is composed of two primary components: hard cost and soft cost.

The hard cost defines whether a cell is traversable or not. Cells that intersect with physical objects or lie within a predefined safety buffer around these objects, are marked as non-traversable, ensuring that the drone avoids any potential collisions. The hard cost $H(i,j,k)$ can be represented as a binary occupancy function as shown in Eq. (1). If the cell is occupied or within the safety margin of obstacles, it will be marked as infinity. Which means it cannot be included in path planning.

$$H(i,j,k) = \begin{cases} \infty, & if\ cell\ occupied \\ 0, & otherwise \end{cases} \quad (1)$$

The soft cost represents the distraction potential or cognitive safety risk associated with drone proximity to human workers. Our previous work showed the drone had less impact on construction workers when flying at 82 ft above the workers [11]. Here, to maintain model tractability, distraction risk was represented as a uniform soft-cost field below this height threshold. Figure 1 shows the definition of distraction areas. The worker distraction area is modelled as the entire construction volume below a height of 82 ft above the highest worker position. Any grid cell located inside the distraction areas is defined as part of the construction worker distraction area. The soft cost $S(i,j,k)$ is defined as Eq. (2). Based on above, the hard cost and the soft cost of the grid cell can be formulated as Eq. (3).

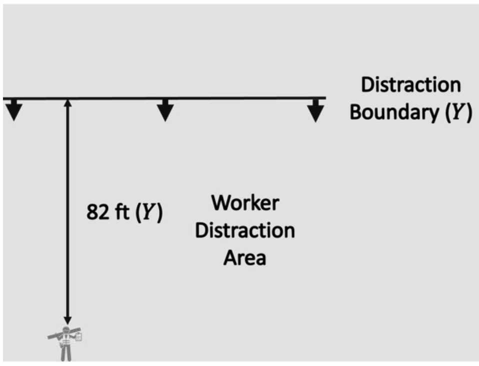

Figure 1. Construction worker distraction areas.

$$S(i,j,k) = \begin{cases} 1 & if\ cell\ in\ distraction\ area \\ 0, & otherwise \end{cases} \quad (2)$$

$$G(i,j,k) = (H(i,j,k) + \lambda * S(i,j,k)) \quad (3)$$

where λ is a weighting coefficient that controls the relative importance of distraction-related soft costs compared to the hard occupancy cost, allowing the planner to balance between path length efficiency and minimizing distraction risks.

3.2 Local Path Planning Module

The Local Path Planning Module computes feasible flight routes between any two travel points within the 3D cost grid. This module employs a greedy search process that explores neighbour grid cells to find a continuous route minimizing the total accumulated cost. In each iteration of the greedy search process, the current grid cell considers 26 neighbour directions in three-dimensional space as potential candidates for the next movement step. These neighbour cells represent all possible moves along the principal axes, face diagonals, and space diagonals. The objective is to reduce the sum of motion and gird (hard and soft) costs across all points, which is to reduce the objective function of Eq. (4). In short, this module provides a sequence of continuous 3D points $P = \{p_0, p_1, \dots, p_n\}$ based on given pair of two traveling points.

$$\min_{p_0,\cdots p_n} A(P) = \sum_{k=0}^{n-1}(t_d(p_k, p_{k+1}) + t_g(p_k, p_{k+1})) \quad (4)$$

$$t_d(p_k, p_{k+1}) = \sqrt{\left(\frac{\Delta x}{v_h}\right)^2 + \left(\frac{\Delta y}{v_v}\right)^2 + \left(\frac{\Delta z}{v_h}\right)^2} \quad (5)$$

$$t_g(p_k, p_{k+1}) = G(p_{k+1}) \times t_{dist}(p_k, p_{k+1}) \quad (6)$$

where v_h and v_v represent the horizontal and vertical flying speeds, respectively.

3.3 Traveling Point Ordering Module

The Traveling Point Ordering Module determines the optimal visiting sequence of all predefined traveling points that the drone must travel with a starting point. This process is formulated as a Traveling Salesman Problem (TSP), the goal is to find the shortest possible route that visits all traveling points once and returns to the starting position. To construct the TSP cost matrix, the pairwise distances between all traveling points are calculated using the Local Path Planning Module described in the previous section. For each pair of points, the local path planner provides not only the feasible route but also the total accumulated cost $A(P)$, which already incorporates both the motion cost and the distraction-related soft cost from Eq. (4). Consequently, the resulting distance matrix inherently reflects obstacle avoidance and distraction-aware constraints within the environment.

Once the distance matrix is constructed, a Nearest-Neighbour heuristic is applied to generate a traveling sequence that reduces the overall travel cost. The heuristic begins from the starting point and iteratively selects the next point that yields the lowest travel cost among the remaining unvisited points. This process continues until all points are visited, forming a complete closed loop that defines the drone's global navigation route.

The final flight route of the drone is obtained by concatenating the locally planned paths between consecutive traveling points according to the optimized visiting order. This hierarchical approach, which integrates local path optimization with global route ordering, enables the drone to achieve efficient, collision-free, and distraction-aware navigation across the construction site.

3.4 Soft Cost Weight Estimation Module

The Soft Cost Weight Estimation module is designed to estimate λ within the 3D cost grid module for use in the local path planning module. The local path planning module serves as the core of the proposed method, incorporating distraction time as a soft cost term to balance path efficiency with distraction avoidance. To achieve this, the soft cost weight estimation module evaluates all possible spatial relationships between the traveling points and the ceiling of the combined distraction area. Since the local path planning module processes two points at a time, three primary conditions are defined:

1. Both points are above the boundary.
2. One point is above the boundary while another is below it.
3. Both points are below the boundary.

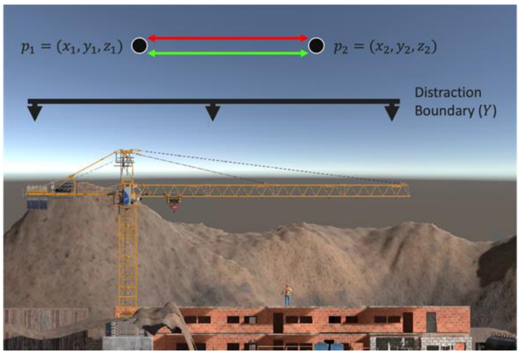

Figure 2. Both points above the distraction boundary.

Figure 2 illustrates the first condition, where both points are located above the ceiling of the distraction area. In this case, the optimal route between points p_1 and p_2 is a direct straight line. The presence or consideration of the distraction area does not affect the path, as the entire route remains outside the distraction area. Thus, the value of soft cost weight (λ) will not affect the path planning in such condition.

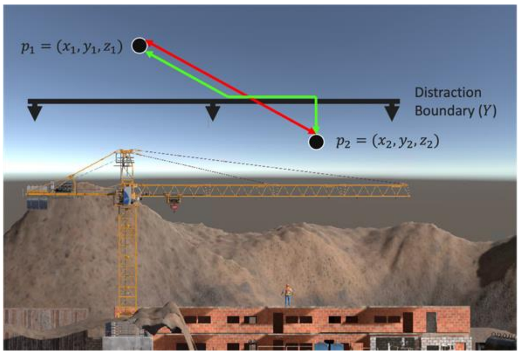

Figure 3. One point above and another point below the distraction boundary.

Figure 3 presents the second condition, where one point is outside and the other is inside the distraction area. The red line represents the optimal route without considering distraction, while the green line shows the optimal route when distraction is taken into account. To enable the proposed method to select the green route, the minimum value of λ can be derived as shown in Eq. (7), ensuring that the cost of the red route is higher than that of the green route.

$$\lambda > \frac{-pdt\left(\frac{y_{p2}}{y_{p1}+y_{p2}}\right)+pdt_h\left(\frac{y_{p2}}{y_{p1}+y_{p2}}\right)+\frac{y_{p2}}{v_v}}{pdt\left(\frac{y_{p2}}{y_{p1}+y_{p2}}\right)-\left(\frac{y_{p2}}{v_v}\right)} \tag{7}$$

$$y_{p1} = |y_1 - Y|, y_{p2} = |y_2 - Y| \tag{8}$$

$$pdt_h = \frac{\sqrt{(x_1-x_2)^2+(z_1-z_2)^2}}{v_h} \tag{9}$$

$$pdt = \sqrt{\left(\frac{x_1-x_2}{v_h}\right)^2 + \left(\frac{y_1-y_2}{v_v}\right)^2 + \left(\frac{z_1-z_2}{v_h}\right)^2} \tag{10}$$

where v_h and v_v represent the horizontal and vertical flying speeds, respectively. x represents horizontal axis and y represents vertical axis.

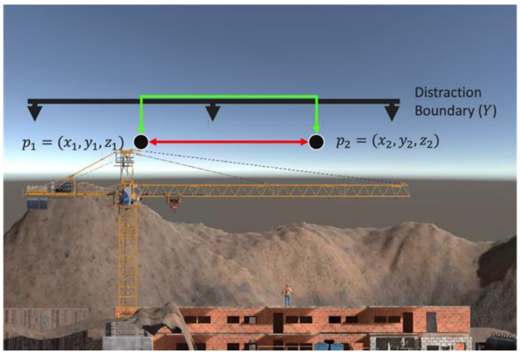

Figure 4. Both points below the distraction boundary.

Figure 4 shows the third condition, where both traveling points are located inside the distraction area. Similar to the previous case, the red line represents the route without considering distraction, and the green line represents the distraction-aware route. To ensure that the proposed method identifies the green route as optimal, the minimum value of λ can be derived as shown in Eq. (11), where the cost of the red route exceeds that of the green route.

$$\lambda > \frac{pdt_h-pdt+y_{p1}+y_{p2}}{pdt-y_{p1}-y_{p2}}, pdt - y_{p1} - y_{p2} > 0 \tag{11}$$

Since multiple spatial relationships may occur among the same set of traveling points, the final estimation of λ is determined as the maximum value calculated from all point pairs using Eq. (7) and Eq. (11). In other words, λ is selected as the largest value among all possible two-point combinations within the set of traveling points, since each of the three equations gives the smallest λ for its respective pair.

4 Preliminary Results and Discussion

The proposed drone path-planning method was implemented and evaluated in a three-dimensional physics-based simulator developed in Unity. The simulator represents a virtual construction environment containing static structures, a tower crane, and a human worker, enabling controlled evaluation of both physical feasibility and distraction-related effects. The drone was programmed to visit predefined waypoints representing inspection or monitoring targets, with a complete flight route computed for each experiment. The horizontal and vertical flight speeds were set to 4.5 mph and 2.25 mph, respectively, to reflect realistic manoeuvring constraints. The 3D cost grid resolution (R) was set to 3.28 ft (1 m), with safety thresholds adjusted accordingly. The worker distraction height threshold was defined as 82 ft plus one grid cell, and the hard-cost collision margin was set to one grid cell, ensuring accurate representation of soft and hard constraints.

Based on the three conditions defined in the Soft Cost Weight Estimation Module, three experiments were designed to evaluate the proposed method. An additional extreme condition was included when Eq. (11) is invalid (i.e. $pdt - y_{p1} - y_{p2} \leq$) to assess the robustness of the approach. In total, four experimental scenarios (Scenes A–D) were evaluated. All scenarios share the same starting location and six traveling points, while differing only in the vertical positions of the points, resulting in varying exposure to worker distraction areas.

- Scene A places all traveling points above the distraction boundary at a height of 144.36 ft (44 m).
- Scene B positions half of the traveling points under the distraction boundary at 128 ft (39 m), while the remaining half are above it at 95.14 ft (29 m).
- Scene C places all traveling points under the distraction boundary at a uniform height of 88.58 ft (27 m).
- Scene D is similar to Scene C but uses an even lower height of 75.46 ft (23 m).

As shown in Figure 5, the traveling points in Scenes A to D share identical horizontal coordinates but differ in elevation, resulting in varying exposure to the worker distraction area. The green marker denotes the common starting point, and the black horizontal line indicates the distraction boundary at 111.55 ft (34 m). The method was evaluated under two configurations: one considering both flight time and distraction-related soft costs ($\lambda > 0$), and one considering flight time only ($\lambda = 0$). Performance was assessed using two metrics: total completion time and time spent within the worker distraction area (distraction time).

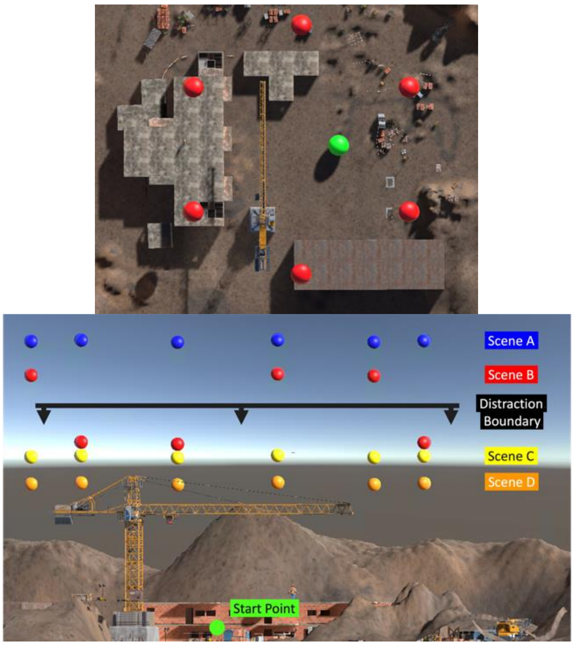

Figure 5. The top view (upper) and the side view (lower) of Scene A and Scene B.

The quantitative results are summarized in Table 1. When the distraction-aware soft cost was included (With Soft Cost), the drone exhibited a tendency to take longer completion time, as indicated by increases in total flight time. However, this behaviour substantially reduced the time spent in distraction area of the construction worker.

Table 1. Comparison of path-planning performance with and without soft cost in Scene A and B.

λ	Scene	Completion time (sec.)	Distraction time (sec.)
0	A	158	61
6.4	A	163	55
0	B	166	86
23.4	B	195	69
0	C	127	127
14	C	190	96
0	D	120	120
20	D	120	120

In Scene A, the total completion time increased by 5 seconds (3.2%), yet the distraction time decreased by 6 seconds (9.8%), with $\lambda = 6.4$. Figure 6 illustrates the route differences between two algorithm configurations in Scene A. From Figure 6 to Figure 9, the red line represents the route generated by the method without considering distraction, while the green line shows the route generated by the method with distraction awareness. As shown in the lower-left part of the figure, the main difference is that the green route ascends vertically when the drone inside the distraction area. This behaviour helps reduced the duration that the drone remains within the distraction area, thereby reducing potential exposure to the worker.

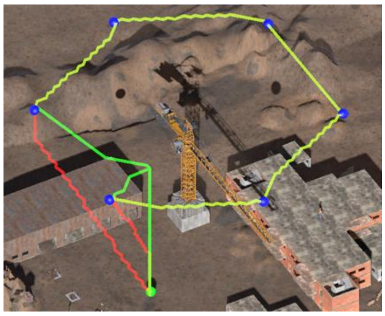

Figure 6. Visualization of planned drone paths with (green) and without (red) soft cost consideration in Scene A. (Yellow line is two lines overlapping)

In Scene B, although the completion time increased by 29 seconds (17.5%), the time spent in the distraction area was reduced by 17 seconds (9.8%), with $\lambda = 23.4$. Figure 7 illustrates the route differences between two configurations in Scene B. Similar to Scene A, the lower-left portion of the figure shows that the distraction-aware method plans a route that moves vertically within the distraction area to reduce the drone's distraction time. In addition, the upper-right, lower-right, and middle-left sections demonstrate that the green route remains above the distraction zone until reaching the vertical position directly above a target point located within the distraction area. The drone then descends straight down to reach the point and ascends vertically afterward to continue to the next destination. This behaviour represents the optimal strategy for reducing the drone's total distraction exposure time.

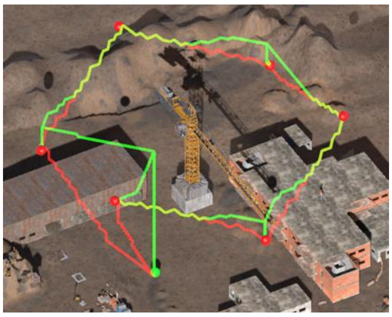

Figure 7. Visualization of planned drone paths with (green) and without (red) soft cost consideration in Scene B. (Yellow line is two lines overlapping)

In Scene C, the completion time increased by 63 seconds (49.6%), while the distraction time decreased by 31 seconds (24.4%), with $\lambda = 14$. Figure 8 illustrates the route differences between the two configurations in Scene C, showing two major distinctions similar to those in Scene B. First, the lower-left portion of the figure shows that the green route moves vertically within the distraction area, unlike the red route. Second, all the traveling points in Scene C are inside the distraction area. Thus, the green route directs the drone to hover directly above each target point, descend straight down to reach it, and then ascend vertically back to the distraction-free area. These behaviours demonstrate the effectiveness of the proposed method in finding an optimal route that reduces distraction time while maintaining the shortest possible completion time under the given objective.

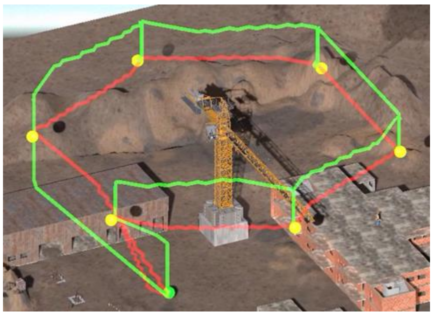

Figure 8. Visualization of planned drone paths with (green) and without (red) soft cost consideration in Scene C. (Yellow line is two lines overlapping)

In Scene D, the path length, completion time, and distraction time were identical across both configurations of the proposed method. Since Eq. (11) was invalid in Scene D, there is no meaningful value of λ that influences or alters the path planning outcome. Here, λ was set as 20 for demonstration. As shown in Figure 9, the green and red routes completely overlap, appearing as a single yellow line. This outcome occurs because all target points are positioned at low elevations, making it inefficient for the drone to ascend to the distraction-free area above each point and descend again. Such unnecessary vertical movements would increase overall distraction time rather than reduce it, resulting in identical optimal routes for both configurations.

Figure 9. Visualization of planned drone paths with (green) and without (red) soft cost consideration in Scene D. (Yellow line is two lines overlapping)

5 Conclusion and Future Work

This study proposed a distraction-aware drone path planning framework with four core modules. The first module is a three-dimensional cost grid that represents hard obstacles and distraction-related soft costs. The second module is a local path planning module that computes paths between travel points while considering both motion cost and distraction cost. The third module is a traveling point ordering module that determines the visiting sequence using a Traveling Salesman Problem formulation. The fourth module is a soft cost weight estimation module that determines appropriate weighting parameters based on the spatial relationships between travel points and distraction boundaries.

Simulation-based evaluations were conducted in a Unity-based virtual construction environment, which provides preliminary validation in controlled settings with a static layout and a single worker. The results indicate that incorporating distraction-related soft costs can reduce the time drones spend within worker distraction areas. Across multiple scenarios, the distraction-aware planning strategy led to moderate increases in total completion time but measurable reductions in distraction exposure. These findings highlight the trade-off between operational efficiency and cognitive safety and suggest that the proposed method can generate feasible flight strategies that reduce worker exposure to distracting drone activity.

In this preliminary study, there are several limitations. For example, a Greedy search strategy was adopted as a lightweight local planner to demonstrate the integration of distraction-related soft costs into drone path planning, with emphasis placed on the distraction-aware cost formulation rather than on benchmarking search algorithms. To enable controlled evaluation in the Unity-based simulation environment, the worker was modeled as a static agent. Moreover, time spent within the distraction area was used as an initial proxy for worker exposure to drone-induced distraction, although this metric does not fully capture broader safety constructs such as situational awareness, hazard recognition, or proximity-based risk.

Future work will compare the proposed framework with more established planners such as A* and Dijkstra, incorporate dynamic worker behavior and more realistic site conditions, and validate the approach through field experiments and real construction site deployments, involving multiple workers, moving equipment, and dynamically changing site conditions. In addition, the distraction-cost model will be refined using graded or dynamic functions that account for drone distance, motion characteristics, visibility, and task context. Broader safety indicators will also be integrated.

References

[1] Wingtra, Why and How to Use Drones in Construction and Infrastructure, (2020). https://wingtra.com/drone-mapping-applications/drones-in-construction-and-infrastructure/.

[2] E. Alvarado, Drones in Construction: a Market Analysis, Drone Industry Insights (2024). https://droneii.com/drones-in-construction-market-analysis.

[3] H. Izadi Moud, A. Shojaei, I. Flood, X. Zhang, M. Hatami, Qualitative and Quantitative Risk Analysis of Unmanned Aerial Vehicle Flights over Construction Job Sites, 2018.

[4] I. Jeelani, M. Gheisari, Safety challenges of UAV integration in construction: Conceptual analysis and future research roadmap, Saf Sci 144 (2021) 105473.

[5] The Wall Street Journal, Drones Are Watching: Railroad Irks Workers With Unmanned Aircraft, (2018). https://www.wsj.com/articles/drones-are-watching-railroad-irks-workers-with-unmanned-aircraft-1521028800 (accessed December 3, 2023).

[6] G. Mark, V.M. González, J. Harris, No task left behind?: examining the nature of fragmented work, Proceedings of the SIGCHI Conference on Human Factors in Computing Systems (2005). https://api.semanticscholar.org/CorpusID:3079084.

[7] M. Khalid, M. Namian, C.C. Massarra, The Dark Side of the Drones: A Review of Emerging Safety Implications in Construction, in: 2021. https://api.semanticscholar.org/CorpusID:237875604.

[8] N. Mostafa, A. Alex, F. Jing, Effect of Distraction on Hazard Recognition and Safety Risk Perception, J Constr Eng Manag 144 (2018) 04018008.

[9] E.M. Altmann, G. Trafton, D.Z. Hambrick, Momentary interruptions can derail the train of thought., J Exp Psychol Gen 143 1 (2014) 215–26. https://api.semanticscholar.org/CorpusID:15459133.

[10] W. Han, L. Xu, M.M. Mouri, W.-Y. Loh, F. Dai, Z. Zhu, Drone-Induced Distraction on Construction Sites: A Quantitative Analysis of Flight Configurations, ISARC. Proceedings of the International Symposium on Automation and Robotics in Construction 42 (2025) 845–852.

[11] W. Han, L. Xu, M.M. Maisha, W.-Y. Loh, F. Dai, Z. Zhu, Drone Flights and Worker Visual Attention: A Quantitative Study of Distraction and Hazard Awareness, J Constr Eng Manag 151 (2025) 04025173.

[12] W. Xu, C. Cui, Y. Ji, X. Li, S. Li, A UAV path planning algorithm for bridge construction safety inspection in complex terrain, Sci Rep 15 (2025) 13564.

[13] J. Zheng, J. Tan, G. Chen, Research on UAV coverage path planning in building visual inspection, Journal of Building Engineering 111 (2025) 113556.

[14] X. Liu, W. Yi, P. Chen, Y. Tan, Flight path planning of UAV-driven refinement inspection for construction sites based on 3D reconstruction, Autom Constr 177 (2025) 106360.

[15] H. Freimuth, M. König, Planning and executing construction inspections with unmanned aerial vehicles, Autom Constr 96 (2018) 540–553.

[16] Y. Huang, A. Hammad, Simulation-Based Optimization of Path Planning for Camera-Equipped UAVs That Considers the Location and Time of Construction Activities, Remote Sens (Basel) 16 (2024). https://doi.org/10.3390/rs16132445.

[17] I. Jeelani, M. Gheisari, Safety Challenges of UAV Integration in the Construction Industry: Focusing on Workers at Height, (2022).

[18] Gilles Albeaino, Idris Jeelani, Masoud Gheisari, Raja R. A. Issa, Attentional Impact of Drones on Construction Sites, Proceedings of 59th Annual Associated Schools 4 (2023) 121–129.

[19] Z. Barlow, H. Jashami, A. Sova, D.S. Hurwitz, M.J. Olsen, Policy processes and recommendations for Unmanned Aerial System operations near roadways based on visual attention of drivers, Transp Res Part C Emerg Technol 108 (2019) 207–222.

[20] D.S. Hurwitz, M.J. Olsen, Z. Barlow, others, Driving Distraction Due to Drones, 2018.

[21] A. Ryan, C. Fitzpatrick, E. Christofa, M. Knodler, Driver performance due to small unmanned aerial system applications in the vicinity of roadways, Transp Res Part F Traffic Psychol Behav 68 (2020) 118–131.